Adsorption mechanism of ferrocene molecular on pristine and functionalized graphene

Nigar, Salma; Wang, Hao; Imtiaz, Muhammad; Yu, Jianshu; Zhou, Zhongfu

Published in:
Applied Surface Science

DOI:
10.1016/j.apsusc.2019.03.222

Publication date:
2019

Citation for published version (APA):
Nigar, S., Wang, H., Imtiaz, M., Yu, J., & Zhou, Z. (2019). Adsorption mechanism of ferrocene molecular on pristine and functionalized graphene. *Applied Surface Science*, *481*, 1466-1473. https://doi.org/10.1016/j.apsusc.2019.03.222

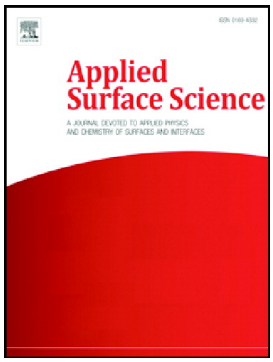

Adsorption mechanism of ferrocene molecule on pristine and functionalized graphene

Salma Nigar, Hao Wang, Muhammad Imtiaz, Jianshu Yu, Zhongfu Zhou

PII: S0169-4332(19)30853-0
DOI: https://doi.org/10.1016/j.apsusc.2019.03.222
Reference: APSUSC 42177

To appear in: *Applied Surface Science*

Received date: 6 November 2018
Revised date: 18 March 2019
Accepted date: 20 March 2019

Please cite this article as: S. Nigar, H. Wang, M. Imtiaz, et al., Adsorption mechanism of ferrocene molecule on pristine and functionalized graphene, Applied Surface Science, https://doi.org/10.1016/j.apsusc.2019.03.222

Adsorption mechanism of ferrocene molecule on pristine and functionalized graphene

Salma Nigar [a], Hao Wang* [a,b,c], Muhammad Imtiaz [d,e], Jianshu Yu[a], Zhongfu Zhou* [a,b,c,f]

[a] School of Material Science and Engineering, Shanghai University, Shanghai 200444, P. R. China

[b] State Key Laboratory of Advanced Special Steel, Shanghai University, Shanghai 200072, P. R. China.

[c] Key Laboratory of Material Microstructures, Shanghai University, Shanghai 200444, P. R. China

[d] State Key Laboratory of Metal Matrix Composites, Shanghai Jiao Tong University, 800 Dongchuan Road, Shanghai 200240, P. R. China

[e] Department of Physics, Islamia College Peshawar, Jamrod Road, Peshawar, Khyber Pakhtunkhwa 25120, Pakistan

[f] Department of Physics, Aberystwyth University, Aberystwyth SY23 3BZ, UK

*Corresponding authors Tel: +86-15221942219. E-mail: z.zhou@shu.edu.cn, zzz@aber.ac.uk

+86-18930980416. E-mail: haowang@i.shu.edu.cn

Abstract

The adsorption behavior and stable geometries of ferrocene molecule on pristine, oxygen and hydroxyl functionalized graphene surfaces are investigated by using first principle density functional calculations based on the PBE-D2 method, which uses GGA-PBE functional with the incorporation of van der Waals (VDW) forces. Our calculations reveal that on all graphene substrates (pristine, oxygen and hydroxyl functionalized), the ferrocene molecule adsorbed with its molecular axis parallel to the surface. Oxygen and hydroxyl functionalized graphene systems have higher adsorption energies, higher charge transfer values and shorter adsorption heights as compared to the pristine graphene. It is concluded that sandwich type π-π interaction along with the van der Waals forces plays a major role in these adsorptions. The physisorption of ferrocene

molecule is supported by the optimized geometrical parameters, adsorption energies and electronic properties. As the activity of a catalyst relies on the controlled adsorption of molecules onto surfaces, we therefore anticipate that these calculations can play an important role in the investigation of catalytic behavior of a catalyst based on the combined systems of graphene and ferrocene molecule. These findings offer more detail investigation of the ferrocene molecule/molecules on different types of graphene surfaces, and we hope that these calculations can open a new way for the upcoming work on other molecules of the metallocene family.

Key words: Pristine graphene, Functionalized graphene, Ferrocene molecule, physisorption, π-π interaction, van der Waals forces

1. Introduction

Ferrocene with the chemical formula $(C_5H_5)_2$ Fe or Cp_2Fe, is an organometallic compound composed of two cyclopentadienyl rings (labeled as Cp) sandwiching an iron atom. The compound was discovered unintentionally and simultaneously by two groups Kealy and Pauson [1] and Miller *et al.* [2] in 1951. Ferrocene and its derivatives due to their peculiar structural, electrical, magnetic, and transport properties are [3, 4] widely used in adhesion processes, catalysis, sensors, solar energy generation, hydrogen storage, cancer therapy, and nano-magnetism [5-8]. For instance, due to its π-electron system, it is getting keen interest from the researchers. These molecules are highly valued as they guarantee high device efficiency. The functioning of the devices relies on the adsorption geometry and the self-assembly of molecules on the substrates. Particularly, the activity of a catalyst can be enhanced by the control arrangement of molecules and their morphological coordination with substrates. However, the

absolute details of the model of the devices and catalysts rooted in ferrocene and graphene combined systems are still insufficient.

The inconsistency is found between the experimental and theoretical calculations about the stability and the favorable adsorption geometries of the ferrocene molecules onto surfaces. Photoemission spectroscopy, electron energy loss spectroscopy (EELS) and nuclear magnetic resonance (NMR) measurements have shown the preferred orientation of ferrocene molecules either with the molecular axis parallel or perpendicular to the surfaces [9-14]. Scanning tunneling microscopy (STM) measurement reveals the dissociative adsorption of the ferrocene molecule on Au (111) surface [15, 16]. Ferrocene is found physisorbed on Cu (111) when its molecular axis is perpendicular to the substrate. Molecules in two adjacent rows adsorbed with a tilt of about 10˚ with respect to each other [17]. However, both vertical and horizontal adsorption geometries of ferrocene molecules were observed on Cu (100) and Cu (111) substrates [18]. Nevertheless, the adsorption behavior and stable geometry of ferrocene molecule on surfaces is still limited.

Since its discovery, graphene has been chosen as a principle material towards adsorption and desorption processes because of its low dimensionality and large surface area to volume ratio [19]. Indeed, molecular adsorption on graphene has been the focus of copious theoretical [20-23] and experimental [24-26] investigations. Due to the physical π-π interaction with a number of chemical species, graphene can be appraised as an appropriate material for catalyst and sensors [27]. Molecular adsorption reveals innovation in the structural, physical and chemical properties of graphene [19, 28]. However, pristine graphene (Pri-Gr) is chemically less reactive, which limits its practical applications in the fields where the interactions with different chemical species are critical. Various techniques such as functionalization, doping and defects are adopted to enhance the reactivity of graphene towards different chemical groups [28-30]. In fact, the

intentional functionalization of graphene with oxygen and hydroxyl group is found as an efficient way to modify its chemical properties [30, 31].

Oxygen and hydroxyl functionalized graphene (O-Gr and OH-Gr) exhibit excellent water solubility, multipurpose surface modification, and fluorescence properties, which are essential for the sensing, detection, and adsorption of molecules. The investigation of the adsorption process of amino acid on oxidized graphene sheet reveals strong interaction between the positively charged constituents of amino acid and the negatively charged oxygen atom of O-Gr. However, the interaction involving the delocalized π-electrons of the aromatic portion of the amino acids and lone-pair electrons of the oxygen atom of O-Gr is very weak [31]. Theoretically, an improvement in the chemisorption of H, OH, and Pt on the O-Gr has been predicted. The further tuning of the reactivity is supposed to rely on the presence of particular oxygen functional groups [32]. Surface modification of graphene by organic molecules could be an effective technique to tailor the electronic structure of graphene. The adsorptions of benzene and naphthalene molecules do not significantly perturb the electronic structure of graphene [33]. However, the interaction of the molecules with graphene was found to increase greatly by the presence of carboxyl groups on the benzene ring [34].

Using density functional theory, we simulate the adsorption of ferrocene molecule on the surface of pristine as well as oxygen and hydroxyl functionalized graphene. We examined the favorable adsorption geometries of ferrocene molecule on the mentioned different graphene surfaces and its impacts on the electronic properties of these surfaces. To the best of our knowledge, there are so far no theoretical studies toward the adsorption mechanism of ferrocene molecule on the surface of pristine, oxygen and hydroxyl group functionalized graphene.

2. Theoretical Methods

All the DFT calculations reported in this study were conducted by using the Vienna *ab-initio* simulation package (VASP) with the projector augmented wave (PAW) basis sets and periodic boundary conditions [35,36]. We performed calculations by the PBE-D2 method, which is PBE empirically including the van der Waals interaction using Grimme's approach [37, 38]. A plane wave basis set is used to expand the wave functions with cutoff energy of 520 eV. The model systems are composed of ferrocene molecule placed on 8×8 supercell (128 atoms) of pristine, oxygen and hydroxyl functionalized graphene. To avoid the interaction between the graphene layer and it's mirror images a vacuum of 20 Å is set between them. Monkhorst−Pack scheme using 5 × 5 × 1 k-points grid is used to sample the first Brillouin zone in reciprocal space. For the density of state (DOS) analysis, a denser, 11×11×1 k-points mesh is used. Band structure is drawn along the high symmetry G-M-K-G directions. All of the configurations including pristine, oxygen and hydroxyl functionalized, and ferrocene adsorbed graphene substrates were fully relaxed by selecting the threshold convergence criteria of 10^{-4} eV and 10^{-2} eV/Å for the total energy and forces respectively. Bader charge analysis computing procedure is used to find out the charge transfer values between the substrate and adsorbate [39]. The equilibrium structures were also analyzed by using a finite displacement approach through the phonopy program. The phonopy code [40] has been used to extract the force constant and to subsequently calculate the phonon dispersion curves and DOS.

The adsorption energy of ferrocene molecule on the all selected graphene surfaces was calculated as:

$$E_{ad} = E_{(f/fu-Gr)} - E_{(fu-Gr)} - E_{(f)} \quad (1)$$

The first term on the right of the equation (1) represents the total energy of the combined ferrocene molecule adsorbed graphene substrates (Pristine or oxygen and hydroxyl functionalized graphene, respectively). Whereas the second term of the equation represents the total energy of isolated or functionalized graphene sheets respectively. The third term stands for the total energy of isolated ferrocene molecule.

3. Results and discussion

Our investigations of the adsorption mechanism of ferrocene molecule on graphene surfaces complement the findings of the preferential adsorption of this molecule on different substrates as reported by various studies [10-13, 17]. Our results reveal that ferrocene molecule adsorbed on pristine and functionalized graphene substrates with its molecular axis parallel to the substrate. These results are in agreement with the adsorption mechanism of ferrocene molecule as demonstrated on Mo (112) substrate [12]. To inspect the adsorption behavior of a ferrocene molecule on pristine graphene, primarily we have developed models for ferrocene molecule, pristine, oxygen and hydroxyl functionalized graphene. To do so, at first we have computed the comparative stability of two conformers of the ferrocene molecule. An eclipsed conformer is found more stable than the staggered one by 0.45 eV. This result is in excellent agreement with the couple-cluster single and double theory CCSD (T) calculation [41]. Secondly, we have carried DFT total energy calculations for Pri-Gr, O-Gr and OH-Gr sheets to determine the optimized parameters (Fig. 1). The calculated bond length (1.42 Å) of Pri-Gr is in accordance with other results [42, 43]. The optimized structure of O-Gr is shown in Fig. 1b. It is observed that the two carbon atoms of graphene bound to an oxygen atom are pulled out of plane in a vacuum with a displacement of 0.46 Å. This corrugation of atoms looks like a ternary ring

closing to an isosceles triangle. Calculations reveal C-O bond length of 1.46 Å. The C-C bond length increased from 1.42 Å to 1.513 Å, which is near to the sp^3 bond length of 1.54 Å [31, 43].

We observe that OH group prefer to adsorb on T-site. Fig. 1c illustrates the optimized structure of OH-Gr. It can be seen that the carbon atoms of graphene near to OH group are pulled out of plane in a vacuum with different displacements. The carbon atom underneath OH group is stretched out of the graphene plane by 0.59 Å. This corrugation of atoms breaks the π bond between two carbons of graphene. This confirms the transformation of sp^2-hybridization of graphene to sp^3. The calculated bond length between graphene (C-atom) and the oxygen atom of the OH group is 1.51 Å, whereas the corresponding O-H bond length is 0.977 Å. Near the adsorbed OH group, the bond length between two carbons of graphene increased from 1.42 Å to 1.50 Å [44, 45].

We also calculate the electronic properties of the considered substrates. The calculated band structure result of Pri-Gr (Fig. S1(a)) is in accordance with other results and confirm that single-layer graphene is a semi-metal [42, 43]. The band structure plot of O-Gr is given in Fig. S1(b), which shows apparent changes near the Fermi level. Dirac structure is destroyed due to the strong hybridization between the orbitals of C and adsorbed oxygen [31]. The shifting of Fermi level of Pri-Gr by 0.06 eV to the valence band is obviously due to the transfer of 0.15 *e* charge from graphene to an adsorbed oxygen atom. All these results reveal the presence of strong interaction between the graphene substrate and an oxygen atom.

The calculated band structure of OH-Gr is given in Fig. S1(c). It can be seen that the adsorption of OH group on graphene leads to significant changes in the electronic structure of Pri-Gr. These changes are evidently due to the covalent bonding between the orbitals of graphene and of O 2S orbital of OH group. Moreover, the shift of the Fermi level (0.2 eV) to lower energy level and

the perturbation of Dirac structure can also be attributed to the strong hybridization between orbitals of C and adsorbed OH group.

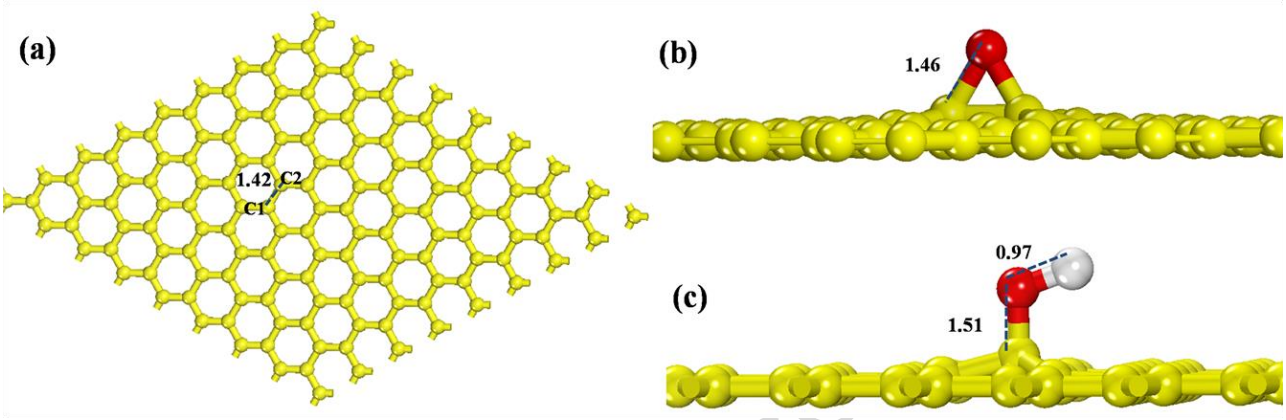

Fig. 1. Optimized structures of (a) pristine (b) oxygen and (c) hydroxyl functionalized graphene.

3.1 Adsorption on pristine graphene (f/Pri-Gr)

To investigate the adsorption behavior of ferrocene molecule on Pri-Gr, we concerned about the favorable adsorption site for ferrocene molecule on the graphene basal plane. Three different adsorption positions i.e. hollow (H), bridge (B) and top of carbon (T) in the hexagon of graphene are selected (Fig. 2a). Ferrocene is oriented with its Fe atom located at directly above these three sites along the z-axis. Our calculations reveal that for ferrocene adsorption, the T-site is the most suitable location. Ferrocene molecule is adsorbed on graphene by selecting two initial adsorption configurations. One is that the molecular axis of the molecule parallel to the surface normal, termed as P-configuration (Fig. 2b) and the other is that the molecular axis perpendicular to the surface normal termed as H-configuration. The H-configuration is further divided into two sub-configurations: (i) only hydrogen atom of each Cp ring is toward the graphene sheet with the

shortest distance from graphene (Hh1) (Fig. 2c) ; (ii) two hydrogen atoms of each Cp ring are toward the graphene sheet with equal distance from graphene (Hh2) (Fig. 2d).

All aforementioned systems with ferrocene approaching the surface of Pri-Gr are fully relaxed, in order to find an appropriate position with the minimum energy. These calculations reveal that ferrocene molecule with Hh2-configuration is the most stable. The energy difference between Hh1 and Hh2-configuration is 0.08 eV. However, the energy difference between the P-configuration and most stable configuration (Hh2) is only 0.023 eV. The robust aspect of our calculation is, that all initial structures with no tilt always relax with the presence of a tilt. The table 1 shows that molecules at P, Hh1 and Hh2-configurations respectively tilted their axis by about 0.2˚, 2.5˚ and 1.2˚ along the surface normal. From table 1 it can also be seen that molecule with P-configuration adsorbed on Pri-Gr surface at an average distance of 3.18 Å. While, the molecule at stable configuration Hh2 adsorbed at an average distance of 2.55 Å. These heights of the molecule from substrates in both configurations are high enough, which supports the weak non-covalent interaction between the adsorbate and substrate [46].

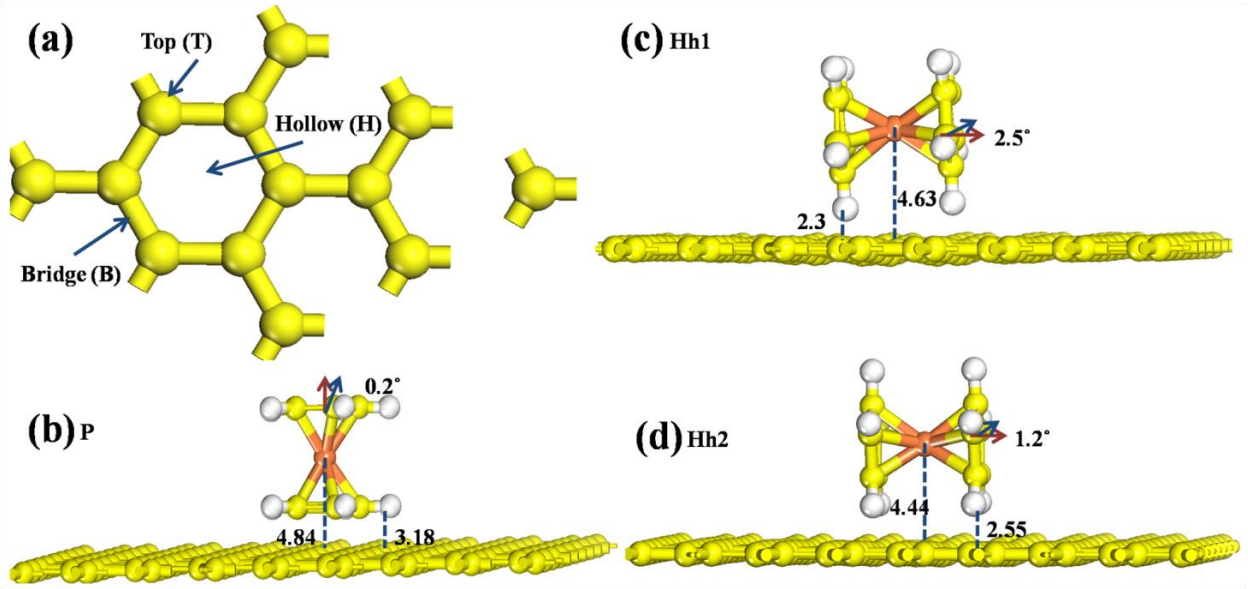

Fig. 2. (a) Favorable adsorption sites i.e. H (hollow), T (top of carbon), B (bridge) on graphene. (b-d) Orientation scheme (optimized structures) for the adsorption of ferrocene molecule on a graphene substrate. P and (Hh1, Hh2) respectively represent P and H-configurations. Here yellow,white and orange balls respectively represent carbon, hydrogen and iron atoms.

Table 1 Adsorption energies (E_{ads}) and optimized structural parameters of the P- and H-configurations of ferrocene molecule on Pri-Gr. The distance of ferrocene molecule from the substrates along the z-axis (h) and (*l*), and tilt degree (ΔΘ). Here (h) represents the distance measured from the top of carbon of graphene to Fe of ferrocene. While (*l*) represents the distance between the lower Cp ring and the graphene sheet.

Configuration	**E_{ads} (eV)**	**Height**		**ΔΘ (deg)**	**Δq (*e*)**
		***h* (Å)**	***l* (Å)**		
P	-0.428	4.84	3.18	0.2	
Hh1	-0.371	4.63	2.3	2.5	
Hh2	-0.451	4.44	2.55	1.2	0.003

3.2 Adsorption on oxygen functionalized graphene (f/O-Gr)

Once we set a benchmark about the stable adsorption site, geometric structure and adsorption energy of f/Pri-Gr, we proceed to the adsorption of ferrocene molecule on oxygen functionalized graphene (f/O-Gr). We aim to explore the adsorption nature, stable geometry and the sensitivity of oxygen modified graphene towards the ferrocene molecule. To do so, both P- and H-configurations are chosen. On the basis of pentagonal shaped rings of ferrocene, different configuring modes such as, Pcph1 (one hydrogen atom per each Cp ring facing an oxygen atom) (Fig. 3a and b), Pcph2 (two hydrogen atoms per each Cp rings facing an oxygen) (Fig. 3c and d), Hcph1(one hydrogen atom per each Cp ring toward the substrate) (Fig. 3e and f) and Hcph2 (two hydrogen atoms per each Cp rings toward the substrate) (Fig. 3g and h) are selected. The calculated adsorption energies, structural parameter and change in angle (tilt) for all mentioned models are displayed in table 2.

For all considered configurations with full relaxation, the horizontal distance of the molecule is changed relative to the oxygen atom in order to approximate an equilibrium position with the lowest energy. The interaction between ferrocene and oxygen atom is found attractive. Wheares, the separating distances in configurations Pcph1, Pcph2, Hcph1 and Hcph2 are 2.40 Å, 2.9 Å, 5.80 Å and 3.86 Å, respectively. The energy difference between Hcph1 and Hcph2 configuration is 0.101 eV. Calculations reveal that Hcph2 is the most stable configuration. In both P- and H-configurations, it is observed that the adsorption energies depend on the distance of separation between an oxygen atom and ferrocene. At a very close distance to an oxygen atom, the interaction is strong repulsive due to the consequence of nucleus-nucleus interaction. This repulsion consequently changes the orientation of ferrocene at different angles. The respective changes (tilt) of the orientational angle of ferrocene in Pcph1, Pcph2, Hcph1 and

Hcph2 are 0.5˚, 0.8˚, 0.1˚ and 0.6˚. Whereas molecule of configurations Hcph1 and Hcph2 are adsorbed at an average distance of 2.3 Å and 2.4 Å respectively. We observed that the adsorption height of ferrocene molecule on O-Gr substrate for the stable configuration Hcph2 is lower than its height on Pri-Gr.

Table 2 The adsorption energy of f/O-Gr (E_{ads}), adsorption height of ferrocene ($h_{f\text{-}Gr}$) and ($l_{f\text{-}Gr}$), bond length between oxygen and carbon ($l_{O\text{–}C}$,), the distance between the oxygen atom and ferrocene molecule ($d_{o\text{-}f}$), change (tilt) in orientation angle of ferrocene (ΔΘ) and charge transfer (Δq). Here ($h_{f\text{-}Gr}$) represents the distance measured from the C of graphene to Fe of ferrocene. Whereas, ($l_{f\text{-}Gr}$) represents the distance of the lower Cp ring from the graphene sheet.

Configuration	**E_{ads} (eV)**	**$h_{f\text{-}Gr}$ (Å)**	**$l_{f\text{-}Gr}$ (Å)**	**$l_{O\text{-}C}$ (Å)**	**$d_{o\text{-}f}$ (Å)**	**ΔΘ (deg)**	**Δq (*e*)**
Pcph1	-0.499	4.82	3.20	1.467	2.4	0.5	
Pcph2	-0.512	4.80	3.17	1.466	2.9	0.8	
Hcph1	-0.416	4.68	2.3	1.46	5.8	0.1	
Hcph2	-0.517	4.34	2.4	1.46	3.86	0.6	0.03

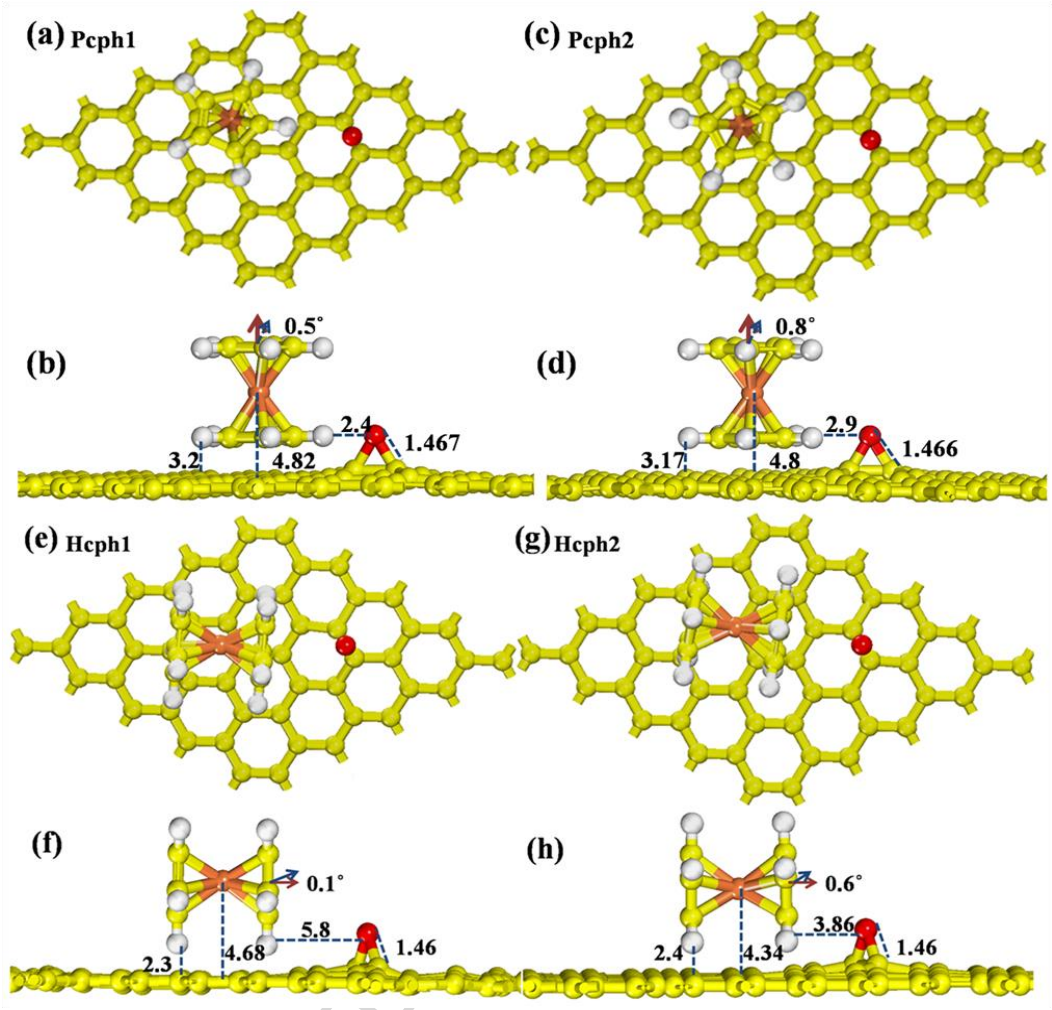

Fig. 3 Adsorption scheme of ferrocene on O-Gr in (a-d) P-configuration and (e-h) H-configuration. (a, c, e and f) top-views and (b, d, f and h) front views of the optimized structures.

3.3 Adsorption on hydroxyl functionalized graphene (f/OH-Gr)

Using the main geometric configurations (P and H), ferrocene molecule is placed on both sides i.e., (a) oxygen and (b) hydrogen of the OH group. The P-configuration is divided into PcpOh1 (one hydrogen of the Cp ring toward the oxygen atom of OH group), PcpOh2 (two hydrogen atoms of the Cp ring toward the O atom of OH group), PcpHh1 (one hydrogen of the Cp ring toward the hydrogen atom of OH group), and PcpHh2 (two hydrogen atoms of the Cp ring toward the hydrogen atom of OH group). These four configurations are shown in Fig. 4a-d.

Correspondingly, the H-configuration is also divided into four different configurations such as HcpOh1 (one hydrogen per each Cp ring toward the graphene), HcpOh2 (two hydrogens per each Cp rings toward the graphene sheet), HcpHh1 (one hydrogen per each Cp rings toward the graphene), and HcpHh2 (two hydrogens per each Cp rings toward the graphene sheet). All aforementioned configurations are shown in Fig. 5a-d.

Following the full relaxation, the distance of the ferrocene molecule is changed relative to both oxygen and hydrogen atoms in order to find an appropriate horizontal separating position with minimum energy. The obtained adsorption energies, optimized structural parameters and change in angle (tilt) for all modeled structure are given in table 3. Calculations reveal that in P-configurations, PcpOh1 is the most stable structure. The molecule is found tilted towards the OH group by 1.8˚(Table 3). The adsorption height of the molecule for PcpOh1-configuration is 4.84 Å (Fe-C distance) and 3.17 Å (lower Cp ring to C of graphene distance). However, in H-configurations, HcpHh2 is found as the most stable configuration. The molecule is found tilted by 2.6˚ towards the OH group. The adsorption heights of the molecule from graphene in HcpHh2-configuration are 4.44 Å (Fe-C distance) and 2.55 Å (average of the nearest neighbor distances between Cp rings and graphene sheet). The comparison of the adsorption energies of PcpOh1 (-0.518 eV) and HcpHh2 (-0.60 eV) show that HcpHh2 is energetically more stable configuration. Moreover, the calculated adsorption energy reveals that the interaction of the ferrocene molecule with the hydroxyl functionalized graphene is stronger than with the pristine graphene.

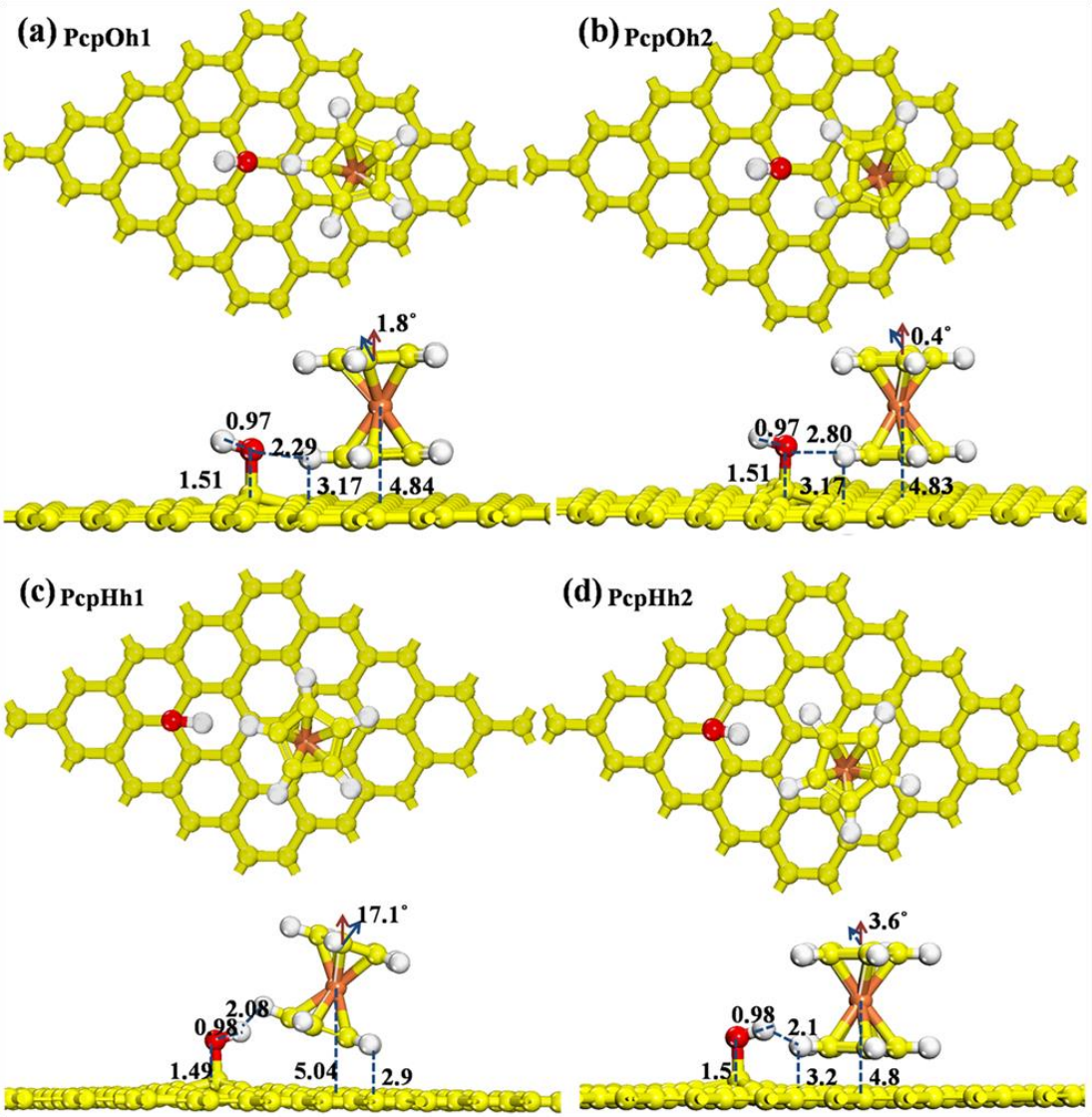

Fig. 4. Adsorption scheme of ferrocene molecule on OH-Gr in P-configuration. The optimized structure of (a) PcpOh1, (b) PcpOh2,(c) PcpHh1 and (d) PcpHh2 [upper panel represents top views while lower one the front views].

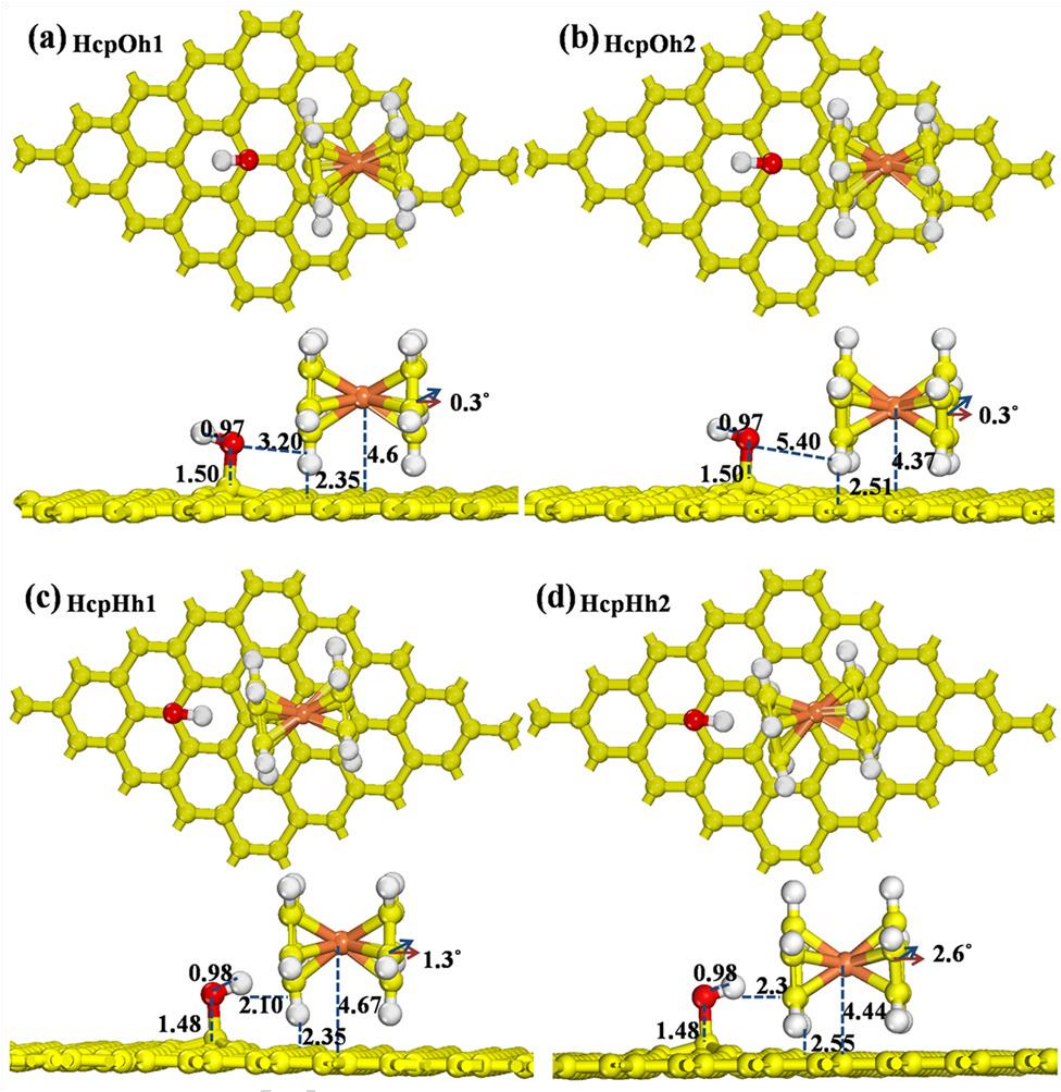

Fig. 5 . Adsorption of ferrocene molecule on OH-Gr in H-configuration: The optimized structure of (a) HcpOh1, (b) HcpOh2, (c) HcpHh1 and (d) HcpHh2 [upper panel represents top views while lower one the front views].

Table 3 The adsorption energy of f/OH-Gr (E_{ads}), distance between OH group and ferrocene molecule (d_{OH-f}), OH–C bond length ($l_{OH–C}$), hydroxyl bond length $d_{(OH)}$, adsorption height of ferrocene (h_{f-Gr}) and (l_{f-Gr}) and height of stretched carbon atom (C_Z) and change in orientation angle (tilt) of ferrocene ($\Delta\Theta$). Here (h_{f-Gr}) represents the distance measured from the C of graphene to Fe of ferrocene. While (l_{f-Gr}) represents the distance of the Cp rings from the graphene sheet.

Configuration	**E_{ads} (eV)**	**d_{OH-f} (Å)**	***l*$_{OH-C}$ (Å)**	**d_{OH} (Å)**	***h*$_{f-Gr}$ (Å)**	***l*$_{f-Gr}$ (Å)**	**C_z (Å)**	**$\Delta\Theta$ (deg)**	**Δq (*e*)**
PcpOh1	-0.518	2.29	1.51	0.97	4.84	3.17	0.57	1.8	
PcpOh2	-0.510	2.80	1.51	0.97	4.83	3.17	0.56	0.4	
PcpHh1	-0.487	2.08	1.49	0.98	5.04	2.9	0.60	17.1	
PcpHh2	-0.498	2.10	1.51	0.98	4.8	3.20	0.53	3.6	
HcpOh1	-0.392	3.20	1.50	0.97	4.6	2.35	0.53	0.3	
HcpOh2	-0.503	5.40	1.50	0.97	4.37	2.51	0.62	0.3	
HcpHh1	-0.578	2.10	1.48	0.98	4.67	2.35	0.53	1.3	
HcpHh2	-0.600	2.30	1.48	0.98	4.44	2.55	0.61	2.6	0.27

3.4 Electronic properties of f/Pri-Gr, f/O-Gr and f/OH-Gr

To further explore the adsorption process in detail, we verify the structure stability of all structures by calculating the phonon dispersion along the first Brillouin zone particularly at Gamma point (Figs. S2-S4, in the supplementary information). The phonon spectrum shows no negative frequencies, which suggests all structures are in stable phase without any dynamical instability. We also calculate the electronic properties of f/Pri-Gr, f/O-Gr and f/OH-Gr systems. The calculated DOS plots of f/Pri-Gr, f/O-Gr, f/OH-Gr and ferrocene molecule (before and after adsorption) are given in Fig. 6a. The band structures of all calculated systems are given in Fig. 6(b-d). The DOS plot of f/Pri-Gr in Fig. 6a shows that a peak appeared near the Fermi level which is obviously caused by the ferrocene molecule states. The analysis of the band structure (Fig. 6b) shows that ferrocene adsorption does not significantly change the band structure of graphene because the Fermi level, shape, and position of the Dirac cone are not changed [24, 33]. However, flat bands appeared below the Fermi level within 0.5 eV, which are due to the development of molecular localized states. The same behavior is observed for f/O-Gr and f/OH-Gr, where no orbital hybridization is observed between the substrates and molecule.

For more detail analysis we show the energy level alignment diagram of graphene and ferrocene molecule before and after adsorption in Fig. 8e and f, respectively. It is clear that the adsorption process does not influence the band structure of pristine graphene. However, it influences the ferrocene molecule. Indeed it shows by the increment or decrement of HOMO and LUMO level of molecular ferrocene, which indicates the achievement of electrical equilibrium. Due to this reason, the semi-metallic band structure of graphene remains same after adsorption. The same mechanism is observed for f/O-Gr and f/OH-Gr. The charge transfer by Bader analysis is 0.003 *e* for f/Pri-Gr, 0.03 *e* for f/O-Gr and 0.27 *e* for f/OH-Gr. These non-significant charge

transfer values also support the reason for the unaltered band structure and electronic properties of graphene. To probe the adsorption features in more detail, we map the isosurface of charge density differences of f/Pri-Gr, f/O-Gr and f/OH-Gr. The plots are given in Fig. S5, which clearly shows that ferrocene molecule stay away from all substrates. This confirms the lack of hybridization and covalent bonding between the orbitals of substrates and molecule [47-49]. These plots support the physisorption of the ferrocene molecule on Pri-Gr.

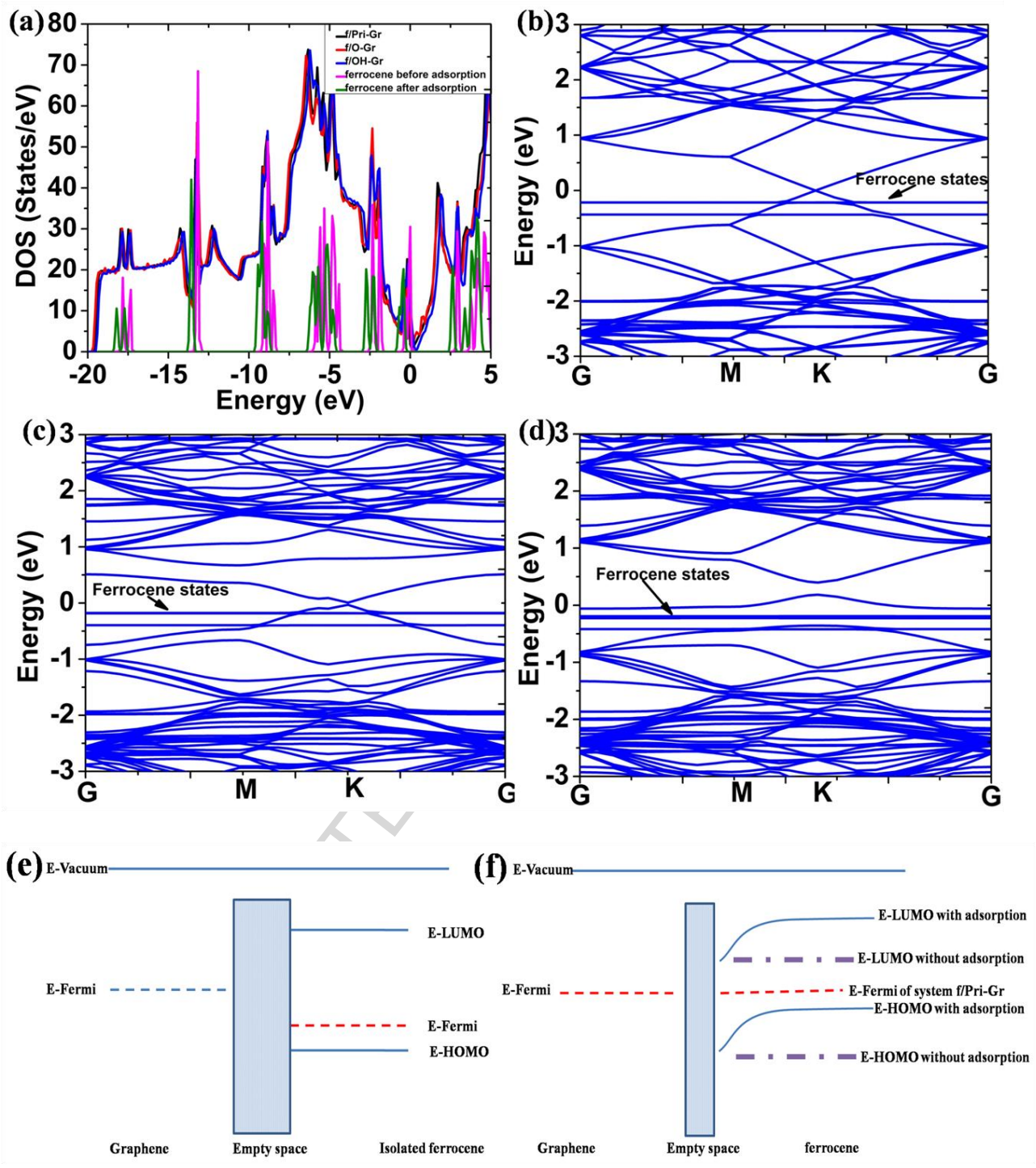

Fig. 6. (a) Calculated DOS of ferrocene adsorbed Pri-Gr, f/O-Gr and f/OH-Gr. DOS of ferrocene before and after adsorption are also given. Band structure of (b) f/Pri-Gr, (c)f/O-Gr and (d) f/OH-Gr. (e) and (f) the band alignment diagram of pristine graphene and ferrocene molecule without and with adsorption process, respectively.

4. Conclusion

Herein, we performed first principle density functional calculations based on PBE-D2 method, to explore the adsorption behavior of ferrocene molecule on pristine, oxygen and hydroxyl functionalized graphene substrates. We found that functionalization of graphene with hydroxyl group presents the greater adsorption stability and charge transfer values; and then followed by the functionalization of oxygen as compared to pristine graphene. On all selected substrates the molecule adsorbs with its molecular axis parallel to the surface. Moreover, the optimized geometrical parameters, adsorption energies and electronic properties show a weak interaction between all substrates and molecule. Therefore, we conclude that the non-covalent sandwich type π-π interaction along with the van der Waals forces is among the fundamental keys of the adsorption of ferrocene molecule on pristine, hydroxyl and oxygen functional graphene. Further investigation for the whole understanding of this adsorption process has already started. And also, these findings offer ample information for the study of the adsorption of ferrocene molecule/molecules or other molecules of metallocene family on other different types of graphene or like surfaces.

Acknowledgments

This research was supported by NSFC (No. 51371112), the innovation program of Shanghai Municipal Education Commission (No. 2014CB643403), and the National Science Fund for Distinguished Young Scholars of China (No.51225401).

References:

[1] T. Kealy, P. Pauson, A new type of organo-iron compound, Nature. 168 (1951) 1039.

[2] S.A. Miller, J.A. Tebboth, J.F. Tremaine, 114. Di cyclo pentadienyliron, J. Chem. Soc. (1952) 632-635.

[3] X. Zhang, J. Wang, Y. Gao, X.C. Zeng, Ab Initio Study of Structural and Magnetic Properties of TM n (ferrocene) n+ 1 (TM= Sc, Ti, V, Mn) sandwich clusters and nanowires (n=∞), ACS nano. 3 (2009) 537-545.

[4] X. Wu, X.C. Zeng, Double Metallocene Nanowires, J. Am. Chem. Soc. 131 (2009) 14246-14248.

[5] Z. Li, Y. Zhao, K. Mu, H. Shan, Y. Guo, J. Wu, Y. Su, Q. Wu, Z. Sun, A. Zhao, X. Cui, C. Wu, Yi. Xie, Molecule-Confined Engineering toward Superconductivity and Ferromagnetism in Two-Dimensional Superlattice, J. Am. Chem. Soc. 139 (2017), 16398−16404

[6] In. H. Kwak, H. G. Abbas,, Ik. S. Kwon, Y. C. Park, J. Seo, M. K. Cho, J. P. Ahn, H. W. Seo, J. Park, H. S. Kang, Intercalation of Cobaltocene into WS2 Nanosheets for Enhanced Catalytic Hydrogen Evolution Reaction. J. Mater. Chem. A, 2019, DOI. 10.1039/C9TA01238A.

[7] L. Fan, Q. Zhang, K. Wang, F. Li, L. Niu, Ferrocene functionalized graphene: preparation, characterization and efficient electron transfer toward sensors of H_2O_2, J. Mater. Chem. 22 (2012) 6165-6170.

[8] F.A. Larik, A. Saeed, T.A. Fattah, U. Muqadar, P.A. Channar, Recent advances in the synthesis, biological activities and various applications of ferrocene derivatives, Appl. Organomet. Chem. 31 (2017) 3664.

[9] Fu-Zhong. Han, Sai-Bo. Yu , C. Zhang , Xiang-Ping. Hu, Chiral ferrocenyl P,S-ligands for highly efficient copper-catalyzed asymmetric [3+2] cycloaddition of azomethine ylides, Tetrahedron. 72 (2016), 2616-2622 .

[10] K. Svensson, T. Bedson, R. Palmer, Dissociation and desorption of ferrocene on graphite by low energy electron impact, Surf. Sci. 451 (2000) 250-254.

[11] Y. Li, X. Chen, G. Zhou, W. Duan, Y. Kim, M. Kim, J. Ihm, Trends in charge transfer and spin alignment of metallocene on graphene, Phys. Rev. B 83 (2011), 195443.

[12] P. Dowben, C. Waldfried, T. Komesu, D. Welipitiya, T. McAvoy, E. Vescovo, The occupied and unoccupied electronic structure of adsorbed ferrocene, Chem. Phys. Lett. 283 (1998) 44-50.

[13] C. Woodbridge, D. Pugmire, R. Johnson, N. Boag, M. Langell, HREELS and XPS Studies of Ferrocene on Ag (100), J. Phys. Chem B. 104 (2000) 3085-3093.

[14] K. J. Cluff, N. Bhuvanesh, J. B. mel, Adsorption of Ruthenium and Iron Metallocenes on Silica: A SolidState NMR Study, Organomet. 33 (2014) 2671−2680

[15] K.-F. Braun, V. Iancu, N. Pertaya, K.-H. Rieder, S.-W. Hla, Decompositional incommensurate growth of ferrocene molecules on a Au (111) surface, Phys. Rev. Lett. 96 (2006) 246102.

[16] R.C. Quardokus, N.A. Wasio, R.P. Forrest, C.S. Lent, S.A. Corcelli, J.A. Christie, K.W. Henderson, S.A. Kandel, Adsorption of diferrocenylacetylene on Au (111) studied by scanning tunneling microscopy, Phys. Chem. Chem. Phys. 15 (2013) 6973-6981.

[17] B. Heinrich, L. Limot, M. Rastei, C. Iacovita, J. Bucher, D.M. Djimbi, C. Massobrio, M. Boero, Dispersion and localization of electronic states at a ferrocene/Cu (111) interface, Phys. Rev. Lett. 107 (2011) 216801.

[18] M. Ormaza, P. Abufager, N. Bachellier, R. Robles, M. Verot, T. Le Bahers, M.-L. Bocquet, N. Lorente, L. Limot, Assembly of ferrocene molecules on metal surfaces revisited, J. Phys. Chem. Lett. 6 (2015) 395-400.

[19] H. H. Gürel, V. O. Özçelik, S. Ciraci, Dissociative Adsorption of Molecules on Graphene and Silicene, J. Phys. Chem. C 118 (2014), 27574−27582

[20] Z. Gaoa, Y. Suna, M. Lia, W. Yanga, X. Dingb, Adsorption sensitivity of Fe decorated different graphene supports toward toxic gas molecules (CO and NO), Appl. Surf. Sci. 456 (2018) 351–359.

[21] C. Han, Z. Chen, Adsorption properties of O_2 on the unequal amounts of binary co-doped graphene by B/N and P/N: A density functional theory study, Appl. Surf. Sci. 471 (2019) 445–454.

[22] W. Zan, Chemical functionalization of graphene by carbene cycloaddition: a density functional theory study, Appl. Surf. Sci. 311 (2014) 377-383.

[23] P. Lazar, F.e. Karlický, P. Jurečka, M.s. Kocman, E. Otyepková, K.r. Šafářová, M. Otyepka, Adsorption of small organic molecules on graphene, J. Am. Chem. Soc. 135 (2013) 6372-6377.

[24] A.S. Rad, O.R. Kashani, Adsorption of acetyl halide molecules on the surface of pristine and Al-doped graphene: ab initio study, Appl. Surf. Sci. 355 (2015) 233-241.

[25] K. Zhang, S. Yu, B. Jv, W. Zheng, Interaction of Rhodamine 6G molecules with graphene: a combined computational–experimental study, Phys. Chem. Chem. Phys. 18 (2016) 28418-28427.

[26] G.e. Yuan, G. Zhang, J. Chen, L. Fu, L. Xu, F. Yang, The electrochemical activities of anthraquinone monosulfonate adsorbed on the basal plane of reduced graphene oxide by π–π stacking interaction, J. Solid. State. Electr. 17 (2013) 2711-2719.

[27] K.-J. Lee, S.-J. Kim, Theoretical investigation of CO_2 adsorption on graphene, Bull. Korean Chem. Soc. 34 (2013) 3022-3026.

[28] Z. Xie, X. Zuo, G.-P. Zhang, Z.-L. Li, C.-K. Wang, Detecting CO, NO and NO_2 gases by Boron-doped graphene nanoribbon molecular devices, Chem. Phys. Lett. 657 (2016) 18-25.

[29] S. Nigar, Z. Zhou, H. Wang, M. Imtiaz, Modulating the electronic and magnetic properties of graphene, RSC. Adv. 7 (2017) 51546-51580.

[30] H. Ren, D.D. Kulkarni, R. Kodiyath, W. Xu, I. Choi, V.V. Tsukruk, Competitive adsorption of dopamine and rhodamine 6G on the surface of graphene oxide, ACS. Appl. Mater. Interfaces. 6 (2014) 2459-2470.

[31] H.T. Larijani, M.D. Ganji, M. Jahanshahi, Trends of amino acid adsorption onto graphene and graphene oxide surfaces: a dispersion corrected DFT study, RSC. Adv. 5 (2015) 92843-92857.

[32] A.S. Dobrota, I.A. Pašti, S.V. Mentus, N.V. Skorodumova, A general view on the reactivity of the oxygen-functionalized graphene basal plane, Phys. Chem. Chem. Phys. 18 (2016) 6580-6586.

[33] A. AlZahrani, First-principles study on the structural and electronic properties of graphene upon benzene and naphthalene adsorption, Appl. Surf. Sci. 257 (2010) 807-810.

[34] A. Rochefort, J.D. Wuest, Interaction of substituted aromatic compounds with graphene, Langmuir, 25 (2008) 210-215.

[35] J.P. Perdew, K. Burke, M. Ernzerhof, Generalized gradient approximation made simple, Phys. Rev. Lett. 77 (1996) 3865.

[36] G. Kresse, J. Furthmüller, Efficiency of ab-initio total energy calculations for metals and semiconductors using a plane-wave basis set. Comput. Mater. Sci. 6, (1996) 15–50.

[37] S. Grimme, Semiempirical GGA-type density functional constructed with a long-range dispersion correction, J. Computat, Chem. 27 (2006) 1787-1799.

[38] D. Mollenhauer, C. Brieger, E. Voloshina, B. Paulus, Performance of dispersion-corrected DFT for the weak Interaction between aromatic molecules and extended carbon-based systems, J. Phys. Chem C. 119 (2015) 1898-1904.

[39] W. Tang, E. Sanville, G. Henkelman, A grid-based Bader analysis algorithm without lattice bias, J. Phys: Condens. Matter. 21 (2009) 084204.

[40] K. Parlinski, First-principle lattice dynamics and thermodynamics of crystals, J. Phys. Conf. Ser. 92 (2007) 012009

[41] S. Coriani, A. Haaland, T. Helgaker, P. Jørgensen, The equilibrium structure of ferrocene, ChemPhysChem, 7 (2006) 245-249.

[42] A.S. Dobrota, I.A. Pašti, N.V. Skorodumova, Oxidized graphene as an electrode material for rechargeable metal-ion batteries–a DFT point of view, Electrochim. Acta. 176 (2015) 1092-1099.

[43] A.C. Neto, F. Guinea, N.M. Peres, K.S. Novoselov, A.K. Geim, The electronic properties of graphene, Rev. Mod. Phys. 81 (2009) 109.

[44] Y. Tang, X. Dai, Z. Yang, L. Pan, W. Chen, D. Ma, Z. Lu, Formation and catalytic activity of Pt supported on oxidized graphene for the CO oxidation reaction, Phys. Chem. Chem. Phys. 16 (2014) 7887-7895.

[45] N. Ghaderi, M. Peressi, First-principle study of hydroxyl functional groups on pristine, defected graphene, and graphene epoxide, J. Phys. Chem C. 114 (2010) 21625-21630.

[46] J. Park, B.D. Yu, S. Hong, Ab initio calculations with van der waals corrections: Benzene-benzene intermolecular case and graphite, J. Korean Phys. Soc, 59 (2011) 196-199.

[47] Y.-H. Zhang, K.-G. Zhou, K.-F. Xie, J. Zeng, H.-L. Zhang, Y. Peng, Tuning the electronic structure and transport properties of graphene by noncovalent functionalization: effects of organic donor, acceptor and metal atoms, Nanotechnology, 21 (2010) 065201.

[48] H. Vovusha, B. Sanyal, Adsorption of nucleobases on 2D transition-metal dichalcogenides and graphene sheet: a first principles density functional theory study, RSC. Adv. 5 (2015) 67427-67434.

[49] S. Gowtham, R.H. Scheicher, R. Pandey, S.P. Karna, R. Ahuja, First-principles study of physisorption of nucleic acid bases on small-diameter carbon nanotubes, Nanotechnology, 19 (2008) 125701.

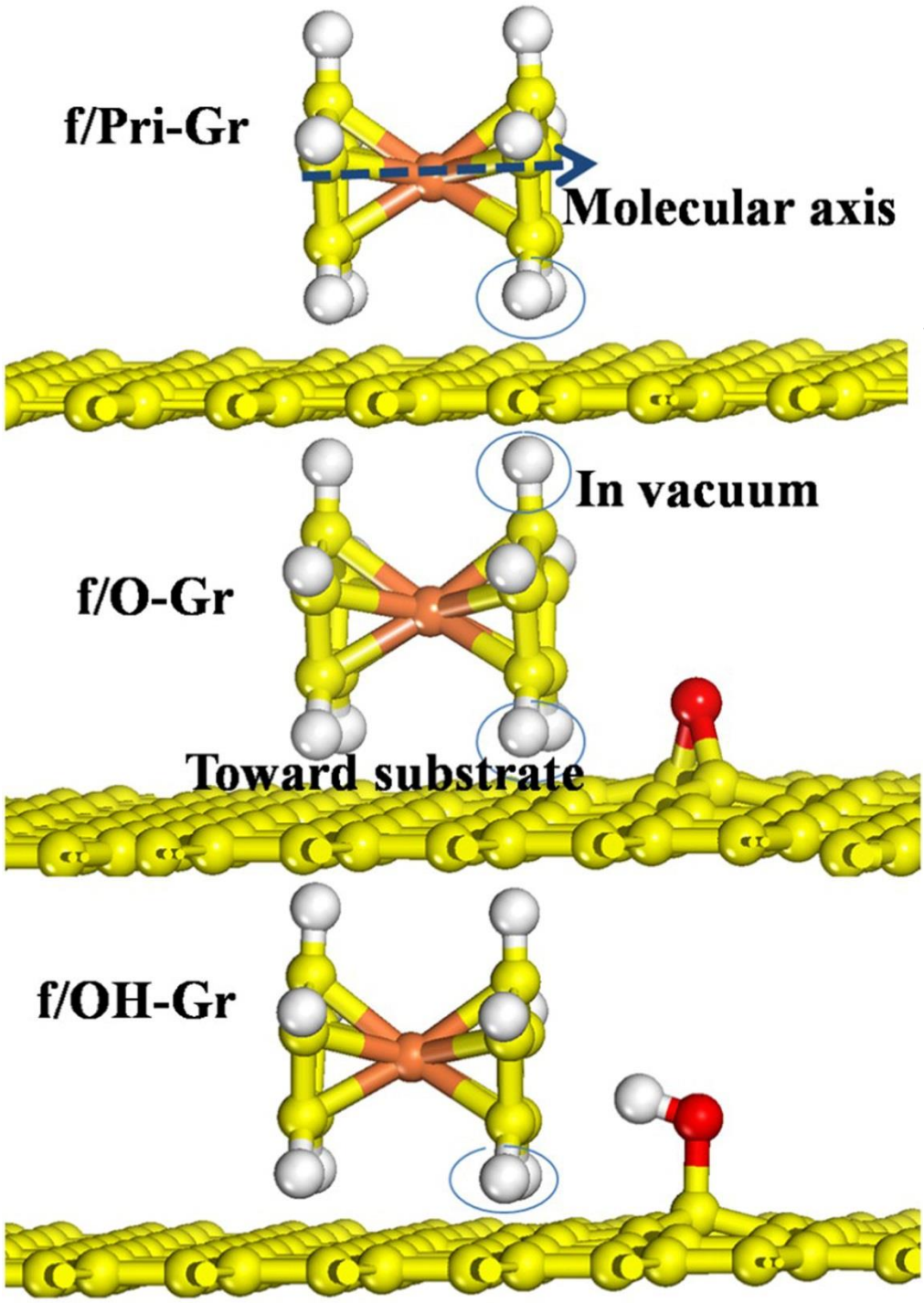

Graphical abstract

Highlights

- Ferrocene molecule physisorbed adsorbed on pristine and functionalized graphene with molecular axis perpendicular to the surface normal.
- The stability of molecule is ensured by the non-covalent π-π interaction and van der Waals forces.
- These calculations are important for the investigation functioning of catalysts based on ferrocene adsorbed graphene.